Published in final edited form as:

J Orthop Res. 2017 September ; 35(9): 1876–1885. doi:10.1002/jor.23502.

ACL injury reduces satellite cell abundance and promotes fibrogenic cell expansion within skeletal muscle

Christopher S. Fry[1], **Darren L. Johnson**[2], **Mary Lloyd Ireland**[2], and **Brian Noehren**[2,3]

[1]Department of Nutrition and Metabolism, University of Texas Medical Branch, Galveston, TX 77555

[2]Department of Orthopaedic Surgery and Sports Medicine, University of Kentucky, Lexington, KY 40536

[3]Division of Physical Therapy, University of Kentucky, Lexington, KY 40536

Abstract

Anterior cruciate ligament (ACL) injuries are associated with significant loss of strength in knee extensor muscles that persists despite physical therapy. The underlying mechanisms responsible for this protracted muscle weakness are poorly understood; however, we recently showed significant myofiber atrophy and altered muscle phenotype following ACL injury. We sought to further explore perturbations in skeletal muscle morphology and progenitor cell activity following an ACL injury. Muscle biopsies were obtained from the injured and non-injured vastus lateralis of young adults (n=10) following ACL injury, and histochemical/immunohistochemical analyses were undertaken to determine collagen content, abundance of connective tissue fibroblasts, fibrogenic/adipogenic progenitor (FAP) cells, satellite cells, in addition to indices of muscle fiber denervation and myonuclear apoptosis. The injured limb showed elevated collagen content ($p<0.05$), in addition to a greater abundance of fibroblasts and FAPs ($p<0.05$) in the injured limb. Fibroblast content was correlated with increased accumulation of extracellular matrix in the injured limb as well. A higher frequency of interstitial nuclei were positive for phospho-SMAD3 in the injured limb ($p<0.05$), providing some evidence for activation of a fibrogenic program through transforming growth factor β following an ACL injury. The injured limb also displayed reduced satellite cell abundance, increased fiber denervation and DNA damage associated with apoptosis ($p<0.05$), indicating alterations within the muscle itself after the ligament injury. Injury of the ACL induces a myriad of negative outcomes within knee extensor muscles, which likely compromise the restorative capacity and plasticity of skeletal muscle, impeding rehabilitative efforts.

Address for correspondence: Brian Noehren, 900 South Limestone Street, University of Kentucky, Lexington, Kentucky 40536-0200, (859) 218-0581 (phone), (859) 323-6003 (fax), b.noehren@uky.edu.

Author contributions: Experiments were performed in the laboratory of CSF. CSF, DLJ, MLI, and BN were involved with conception and design of the experiments; CSF and BN collected, analyzed and interpreted the data; CSF, DLJ, MLI, and BN were involved with drafting the article and revising it critically for important intellectual content. All authors read and approved the final version of the manuscript.

Keywords

CD56; fibroblast; FAP; collagen; anterior cruciate ligament

Introduction

Over 200,000 anterior cruciate ligament (ACL) tears are estimated to occur annually in the United States[1; 2]. The injury is associated with profound loss in quadriceps strength which may not fully recover despite surgery and extensive physical therapy[3–14]. The persistent quadriceps weakness impairs the patient's ability to return to their prior physical activity levels[9; 15; 16]. To date, little is understood of the underlying alterations in muscle physiology as the result of having an ACL tear. We have recently shown that muscle satellite cell abundance declines and there is an expansion of the extracellular matrix (ECM) after an ACL tear[17]. However, it remains unknown whether these changes are accompanied by myonuclear apoptosis or fiber denervation. Additionally, greater characterization of the ECM composition and the effect of ACL tear on muscle interstitial cells responsible for ECM biosynthesis has not yet been defined.

Examining the effect of ACL injury on collagen accumulation in the connective matrix and myonuclear turnover will provide crucial information on the plasticity of skeletal muscle[18]. These deleterious alterations diminish muscle adaptation and may hinder recovery following ACL injury. Fibroblasts contribute to the excessive production of ECM components that can perpetuate into pathological muscle fibrosis[19]. Muscle connective tissue fibroblasts can be identified by their expression of the Tcf4 transcription factor[18; 20], and are observed in areas of ECM accumulation within the muscle. Additionally, the pathological accumulation of connective tissue has recently been linked to mesenchymal-derived fibrogenic/adipogenic progenitors (FAPs)[21; 22], which express the platelet-derived growth factor receptor α (PDGFRα) surface marker[23]. In conjunction with myonuclear apoptosis and our previous report of reduced satellite cell abundance, these maladaptations can contribute to a negative environment for muscle growth[17]. Therefore, the purpose of this study was to define the incidence of myonuclear apoptosis, as well as alterations in the ECM due to FAPs and fibroblasts in the injured and non-injured limbs of human subjects with an ACL tear. We hypothesized that the ACL tear would result in greater frequency of fiber denervation, increased collagen content, increased fibroblast and FAP abundance, and increased myonuclear apoptosis.

Methods

Study Design

Subjects provided their written informed consent from a protocol approved by the institutional review board at the University of Kentucky in accordance with the standards set by the latest revision of the Declaration of Helsinki. This is a case-control study, indicative of level 3 evidence. To qualify for the study subjects could not have undergone ACL reconstruction or had any previous ACL reconstructions or tears other than the current injury. Subjects were excluded if they had a total knee dislocation. The diagnosis of the ACL

injury was made by one of two orthopedic surgeons using routine physical examination and magnetic resonance techniques. We have previously used the same cohort to investigate the effect of an ACL injury and reconstruction on muscle fiber type and atrophy[17]. Based upon the finding of our initial report, it led us to conduct additional analyses on fibrogenic cell expansion and fiber denervation in the same subjects; however, data presented here have not previously been reported.

Muscle biopsies from the injured and non-injured limbs were collected during the same visit for each subject. Percutaneous muscle biopsies were then sampled from the *m. vastus lateralis* using a Bergström 5 mm muscle biopsy needle with suction. Samples were dissected free of connective tissue, oriented properly, mounted in tragacanth gum on cork and flash frozen in liquid nitrogen-cooled 2-methylbutane. Samples were then transferred to storage at −80°C until processing.

Histochemistry and immunohistochemistry

Seven μm thick sections were cut in a cryostat (HM525, ThermoFisher, Waltham, MA), and sections were allowed to air dry for 1 h. Immunohistochemical techniques were conducted as previously described[18; 24; 25]. For collagen staining, slides were fixed 1 h at 56°C in Bouin's fixative then incubated in picro-sirius red, washed in 0.5% acetic acid, dehydrated, equilibrated with xylenes and then mounted with cytoseal XYL (Thermo Scientific).

For Tcf4/wheat germ agglutinin staining (WGA), slides were fixed in 4% paraformaldehyde followed by epitope retrieval using sodium citrate (10 mM, pH 6.5) at 92°C for 20 min. Endogenous peroxidase activity was blocked with 3% hydrogen peroxide in PBS for 7 min. Slides were incubated overnight in anti-Tcf4 (#2569; Cell Signaling, Danvers, MA) and AF488-conjugated WGA (#W11261; ThermoFisher). The following day, slides were incubated in goat anti-rabbit biotin secondary antibody (#111-065-003; Jackson Immuno Research, West Grove, PA) for 1 h, and reacted with streptavidin–horseradish peroxidase and AF555 tyramide included with the TSA kit (#T20935, Life Technologies). Slides were co-stained with DAPI prior to being mounted with fluorescent mounting media.

For PDGFRα/WGA, slides were fixed in 4% paraformaldehyde, and incubated overnight in anti-PDGFRα (#AF-307-NA; R&D Systems, Minneapolis, MN) and AF488-conjugated WGA. The following day, slides were incubated in rabbit anti-goat AF555 (#A-21431, ThermoFisher), co-stained with DAPI, and then mounted with fluorescent mounting media.

For PDGFRα/Tcf4, slides were fixed in 4% paraformaldehyde followed by epitope retrieval using sodium citrate. Endogenous peroxidase activity was blocked with 3% hydrogen peroxide, and slides were incubated overnight in anti-Tcf4 and anti-PDGFRα. The following day, slides were incubated in donkey anti-rabbit biotin secondary antibody (#711-065-152; Jackson Immuno Research) and chicken anti-goat AF594 (#A-21468; ThermoFisher) for 1 h, and reacted with streptavidin–horseradish peroxidase and AF488 tyramide included with the TSA kit (#T20932, Life Technologies). Slides were co-stained with DAPI prior to being mounted with fluorescent mounting media.

For p-SMAD3/dystrophin, slides were fixed in 4% paraformaldehyde followed by epitope retrieval using sodium citrate (10 mM, pH 6.5) at 92°C for 20 min. Slides were incubated overnight in anti-p-SMAD3 (#9520; Cell Signaling) and anti-dystrophin (#VP D505; Vector Laboratories, Burlingame, CA). The following day, slides were incubated in goat anti-rabbit AF555 (#A-21429) and goat anti-mouse AF488 (#A-21121), both from ThermoFisher, then co-stained with DAPI and mounted with fluorescent mounting media.

For terminal deoxynucleotidyl transferase dUTP nick end labeling (TUNEL)/dystrophin staining, slides were fixed in 4% PFA for 10 min and then incubated in the In Situ Cell Death Detection Kit (#11684817910; Roche, Indianapolis, IN) per manufacturer instructions. Slides were then blocked in 2.5% normal horse serum (#S-2012; Vector Labs) and incubated in anti-dystrophin (#VP-D505; Vector) overnight. The following day, slides were incubated in goat anti-mouse AF555 (#A-21127; ThermoFisher) and then co-stained with DAPI prior to being mounted with fluorescent mounting media.

For CD56 (Neural Cell Adhesion Molecule [NCAM])/MyHC type 1/laminin staining, slides were fixed for 10 min in ice-cold acetone, and then slides were incubated overnight in anti-laminin (#L9393; Sigma Aldrich, St. Louis, MO) and anti-myosin heavy chain (MyHC) type 1 antibodies (#BA.D5; IgG2b, Developmental Studies Hybridoma Bank, Iowa City, IA) at 4°C. The next day, slides were incubated in goat anti-rabbit AF488 (#A-11034; ThermoFisher) and goat anti-mouse IgG2b, AF647 (#A-21242; ThermoFisher) for 1 h and then blocked for 1 h in 2.5% normal horse serum (#S-2012, Vector). Slides were incubated overnight at 4°C in anti-CD56/NCAM antibody (#555514; BD Biosciences, San Jose, CA), followed by goat anti-mouse AF555 (#A-21127, ThermoFisher). Slides were co-stained with DAPI prior to being mounted with fluorescent mounting media.

Image acquisition and analysis

Images were captured at 100 – 400× total magnification at room temperature with a Zeiss upright microscope (AxioImager M1, Oberkochen, Germany) and analysis carried out using the AxioVision Rel software (v4.9). Image analysis was performed in a blinded manner, where the assessor did not know if the image was from the injured or non-injured limb. WGA and picro-sirius red staining were quantified to measure expansion of the extracellular matrix and collagen between muscle fibers using the thresholding feature of the AxioVision software, and the area occupied by WGA and collagen was expressed relative to the total muscle area (mm^2). Fibroblasts were identified as Tcf4+ / DAPI+ and residing within the interstitial space between fibers. FAPs were identified as PDGFRα+ / DAPI+ and residing within the interstitial space between fibers. Fibrogenic cells were additionally analyzed for dual expression of PDGFRα / Tcf4 in addition to a co-stain with DAPI. A subset of Tcf4+ cells concurrently expressed PDGFRα, while other Tcf4+ cells were PDGFRα−. Myonuclei undergoing apoptosis were identified as TUNEL+ / DAPI+ and residing within the dystrophin border. p-SMAD3+ myonuclei and interstitial cells were identified as p-SMAD3+ / DAPI+. A nucleus was identified as a myonucleus if it met one of the following criteria: 1) it was clearly located within the dystrophin boundary; 2) it was on the boundary facing inside the fiber; or 3) >50% of the area fell inside the dystrophin boundary, as previously reported[26]. Fiber type-specific satellite cell abundance was assessed using CD56

staining in conjunction with MyHC type I/laminin, and only those loci that were scored as CD56+ and DAPI+ within the laminin border were counted. Fiber types were scored as MyHC Type 1+ (Type 1) or MyHC Type 1− (Type 2). NCAM+ denervated fibers were quantified by ubiquitous expression of NCAM (CD56) throughout the fiber.

Statistical analysis

Data are presented as mean ± SEM. Paired samples student's t-tests were performed to compare each dependent variable (Injured vs Non-injured) with $P \leq 0.05$. Comparison of outcomes by injury status and fiber type or injury status and PDGFRα/Tcf4 staining were analyzed using a two factor ANOVA with $P \leq 0.05$. Assumptions for the student's t-test and ANOVA were met (normally distributed data and approximately equal variance) with the exception of TUNEL/dystrophin staining results (data were not normally distributed). TUNEL/dystrophin results were analyzed using a Wilcoxon signed-rank test with $P \leq 0.05$. Simple correlations were tested by assessing the existence of a linear fit between appropriate outcome measures (Tcf4+ fibroblasts/PDGFRα+ FAPs and ECM). All analyses were performed with SigmaPlot 12.0 (Systat Software, San Jose, CA).

Results

Subject characteristics

Eight males and two females (average: age 23±5 yr, weight 78±13 kg, and height 1.77±0.08 m) with ACL tears completed the study. The average time from injury to completing the biopsies was 59±67 days. There was no significant relationship between the time from injury to biopsy and any of the outcome variables (data not shown). Time from injury to biopsy displayed a trend for a positive linear relationship with NCAM+ fiber frequency ($R^2 = 0.28$, $p = 0.08$).

Alterations in muscle connective tissue and fibrogenic cell abundance following ACL injury

Skeletal muscle collagen content was determined through picro-sirius red staining and demonstrated increased accumulation in the injured limb ($p < 0.05$, Figure 1). Collagen content was approximately two fold greater in the interstitial space between fibers in the injured compared to the non-injured limb. In addition to increased collagen accumulation, histological examination suggested cellular infiltration within the ECM in the injured limb. As the observed mononuclear cells appeared to be embedded in the ECM, Tcf4 immunohistochemistry was performed to identify muscle fibroblasts (Figure 2A–B). Tcf4+ fibroblasts were located in the extracellular space surrounding muscle fibers, specifically in areas of collagen accumulation (Figure 2B). Within the injured limb, the number of muscle fibroblasts was higher ($p < 0.05$) (Figure 2C), consistent with the increase in muscle collagen deposition. Additionally, Tcf4+ fibroblast abundance correlated strongly with ECM accumulation within the injured limb (Figure 2D).

The pathological accumulation of connective tissue has recently been linked to fibrogenic/adipogenic progenitor (FAP) cells[21], which express the PDGFRα surface marker[23; 27]. Immunohistochemical quantification of PDGFRα+ cells (Figure 3A–B) demonstrated

elevated abundance within the muscle of the injured limb compared to the non-injured limb ($p < 0.05$, Figure 3C). As with Tcf4+ fibroblasts, the abundance of FAPs was positively correlated with ECM accumulation within the injured limb (Figure 3D). PDGFRα-expressing cells also expressed Tcf4, but not all Tcf4+ cells expressed PDGFRα (Figure 4A–D). We observed an interaction ($p < 0.05$) between ACL injury and PDGFRα/Tcf4 staining. Specifically, the relative proportion of Tcf4+ cells that did not express PDGFRα was greater in the injured limb muscle ($p < 0.05$, Figure 4E).

Both fibroblasts and FAPs increase biosynthesis of ECM components, including collagens, following exposure to transforming growth factor (TGF) β, which transduces its activity through phosphorylation of the transcriptional co-activator SMAD3 to regulate gene expression. To assess the activity of the TGF-β – SMAD3 signaling pathway, we used p-SMAD3 immunohistochemistry and DAPI staining to identify myonuclei and interstitial nuclei that were positive for p-SMAD3 (Figure 5A). Within the injured limb muscle, there was a trend for an increased proportion of p-SMAD3+ myonuclei ($p = 0.06$, Figure 5B) and a statistically significant increase in the proportion of p-SMAD3+ interstitial nuclei ($p < 0.05$, Figure 5C).

Increased myonuclear apoptosis, reduced satellite cell abundance and increased frequency of fiber denervation following an ACL injury

Inactivity and improper activation following injury burdens muscle fiber homeostasis and may lead to DNA damage within myonuclei. DNA damage associated with apoptosis was detected immunohistochmically with TUNEL and dystrophin staining (Figure 6A–D). An increased frequency of myonuclear apoptosis (TUNEL+ myonuclei residing within the dystrophin-labeled sarcolemma) was observed in the muscle of the injured limb compared to the non-injured limb ($p < 0.05$, Figure 6E–F).

We have previously shown reduced abundance of Pax7+ satellite cells following an ACL injury[17]. Human muscle satellite cell content is also commonly assessed with CD56[28; 29], and we determined CD56+ satellite cell content in a fiber type-specific manner in the current study (Figure 7A–E). We observed a main effect of the ACL injury on reduced CD56+ satellite cell abundance in both MyHC type 1 and 2 fibers, in addition to a main effect of fiber type on CD56+ satellite cell content ($p < 0.05$, Figure 7F). Pooling CD56+ satellite cells irrespective to fiber type demonstrated a ~40% reduction in number in the injured limb ($p < 0.05$, Figure 7F), similar to previous reports using Pax7 to quantify satellite cells[17].

In addition to serving as a marker for satellite cells, CD56 or NCAM has also been used to identify denervated muscle fibers in animals[30] and humans[28; 31]. NCAM+ muscle fiber frequency (Figure 7A–E) demonstrated a main effect of ACL injury in both MyHC Type 1 and 2 fibers ($p < 0.05$, Figure 7G). Skeletal muscle in the injured limb had a higher frequency of NCAM+ fibers when pooled irrespective to fiber type as well ($p < 0.05$; Figure 7G).

Discussion

Anterior cruciate ligament tears result in a significant loss of quadriceps strength which may not fully recover. Our findings extend what is known by showing that soon after an ACL tear the vastus lateralis muscle has elevated collagen content, increased fibroblast and FAP abundance, in addition to a greater frequency of p-SMAD3 positive nuclei. A concurrent reduction in satellite cell abundance and increased indices of muscle fiber denervation and myonuclear apoptosis were also observed in the injured limb muscle. These results show that that an ACL tear is associated with negative alterations that impede the muscles' ability to regenerate and maintain strength.

We have previously reported that there is an expansion of the ECM following an ACL injury[17]. Our current results show that the observed expansion of the ECM is the result of greater collagen deposition. Collagen accumulation likely increases the stiffness of the ECM surrounding muscle fibers, potentially limiting muscle fiber hypertrophy[32]. Increased collagen content may be potentially beneficial for the transmission of force to the tendon encapsulating the muscle fibers; however, excess fibrotic material may hinder muscle fiber hypertrophy and/or retard the ability of satellite cells to leave the basal lamina and enter the fiber during repair/growth[32]. Additionally, the expansion of the ECM and increased matrix stiffness can negatively affect satellite cells through reduced proliferation and self-renewal[33–36]. This could be one potential factor contributing to long term strength reductions following an ACL injury. Consistent with the expansion of the ECM we found a significant elevation of PDGFRα+ FAPs[27]. FAPs have been shown to be elevated in other more severe musculoskeletal diseases characterized by pathological fibrosis such as Duchenne muscular dystrophy[37]. To the best of our knowledge, this is the first report showing elevated FAP content in association with a moderate expansion of the ECM, providing support for a role for FAPs in skeletal muscle following a variety of injuries. Resistance training promotes proliferation of FAPs[38], and interaction between FAPs and satellite cells stimulates myogenesis[39], which would promote positive adaptations following injury. While genetic overexpression of PDGFRα can drive systemic fibrosis in a number of tissues[23], the interaction of FAPs and satellite cells is critical in the regenerative response following an acute injury[39]. Proper regulation of FAP activity is likely crucial in the homeostatic maintenance of skeletal muscle ECM, preventing overproduction and accumulation of ECM components which could adversely affect muscle architecture and function. The acute activation of FAPs following injury can be beneficial, with ECM biosynthesis providing scaffolding for muscle formation; however, chronically elevated FAP content likely reduces muscle quality and must be kept in check. Our results provide evidence for a prolonged elevation in FAP content within the injured limb muscle, which may be contributing to the accumulation of intramuscular collagen.

Concurrent with elevated FAP content, we also observed greater abundance of Tcf4+ muscle connective tissue fibroblasts within the injured limb. The Tcf4 transcription factor has been used as a marker of connective tissue fibroblasts in murine skeletal muscle[18; 20; 40], and we show that Tcf4 labels mononuclear cells residing in the interstitial space between muscle fibers in human skeletal muscle. We observed an accumulation of Tcf4+ cells within areas defined by greater ECM density in the vastus lateralis following ACL injury and

reconstruction. While an in-depth profile of human Tcf4+ cells was not performed in the current study, it is likely that the Tcf4 transcription factor specifies a population of connective tissue fibroblasts, as it does in murine muscle. Tcf4+ fibroblasts contribute to muscle adaptation, during both regeneration[20] and hypertrophy[18]. Prolonged expansion or unchecked proliferation of the Tcf4+ fibroblast pool can have deleterious effects on both regeneration and hypertrophy through expansion of the ECM that likely impedes myogenesis and muscle fiber growth[18; 20]. Indeed, Tcf4+ fibroblast content was positively correlated with ECM accumulation in the injured limb muscle, providing support for an integral role of connective tissue fibroblasts in the biosynthesis of ECM components. Increases in fibroblast content and ECM accumulation likely limit muscle plasticity and may negatively impact rehabilitative efforts, contributing to the protracted muscle weakness that is associated with ACL injury.

Recent work in mouse skeletal muscle following injury shows that both FAPs and Tcf4+ fibroblasts express PDGFRα, suggesting that these populations might be overlapping[41]. However, a direct relationship between PDGFRα+ progenitors and Tcf4+ fibroblasts has not been definitively demonstrated[42]. We show in human muscle that cells expressing PDGFRα concurrently express Tcf4, but a larger subset of Tcf4+ cells do not express PDGFRα. Additionally, cells positive for Tcf4 only were elevated in the injured limb. This may indicate a preferential transition to a more fibroblast-like phenotype from the progenitor FAP following ACL injury. Future experiments are needed to explicitly compare the relationship between Tcf4+ fibroblasts and PDGFRα+ FAPs following an ACL injury.

TGF-β can promote the proliferation and enhance ECM biosynthesis in both connective tissue fibroblasts[43] and FAPs[21]. In the current study, we utilized nuclear co-localization of p-SMAD3, a downstream effector of TGF-β, as a proxy for TGF-β activity within interstitial cells, some of which are likely fibroblasts and FAPs. The frequency of interstitial nuclei (those residing outside of the dystrophin border) that were positive for p-SMAD3 was elevated in the injured limb compared to the non-injured control. The increase in p-SMAD3+ interstitial nuclei provides some evidence for TGF-β-mediated stimulation of fibrotic cell proliferation and increased collagen content within the muscle. Future research will explore the contribution of TGF-β in the development of connective tissue accumulation and fibrotic cell abundance following an ACL injury and reconstruction.

Our previous work identified a reduction in Pax7+ satellite cells following ACL reconstruction[17], and these results are confirmed in the current study, as CD56+ satellite cell abundance is reduced in the injured limb following ACL injury. Following injury or during adaptation, myonuclear addition within muscle fibers is accomplished solely through the activation and fusion of satellite cells[44; 45]. Reductions in satellite cell abundance may mitigate muscle fiber hypertrophy and impede rehabilitation of the injured limb. While genetic models have shown that short-term muscle hypertrophy can occur independently of satellite cell fusion[44; 46], long term growth is attenuated[18], supportive of satellite cell-mediated contributions to muscle adaptation. Additionally, satellite cells interact with Tcf4+ fibroblasts during hypertrophy and regeneration after injury to regulate proper ECM remodeling, and reductions in satellite cell content have been shown to promote Tcf4+ fibroblast expansion and ECM accumulation[18; 20; 47]. The observed decline in satellite cell

abundance following ACL injury and reconstruction may promote fibroblast proliferation and subsequent collagen accumulation within the injured limb muscle. While the cause of the satellite cell decline is not readily apparent, it also can reduce the regenerative capacity of the injured limb muscle. If rehabilitative efforts induce damage to the muscle, adequate repair and recovery may be compromised, stymieing rehabilitative efforts.

We have previously reported a shift in myosin heavy chain expression following ACL reconstruction[17], and in the current study, we show that following an ACL injury a small, but significant elevation in the frequency of NCAM+ muscle fibers is observed in the injured limb. NCAM expression has been used to quantify fiber denervation in both rodents[30] and humans[31]. Fiber denervation status is modulated by inactivity[28] and resistance training[48] in humans, and results from the current study would indicate that an ACL injury may increase the frequency of denervated muscle fibers. Increased fiber denervation may contribute to knee extensor weakness following ACL injury, in addition to reported muscle atrophy[17]. ACL injury may also promote myonuclear turnover, as indicated by the frequency of TUNEL+ myonuclei observed in the current study. Four of our ten subjects displayed evidence for myonuclear apoptosis which may promote muscle atrophy and likely places patients at a disadvantage when attempting to rehabilitate knee extensor muscles in the injured limb. Myonuclear accrual is a key predictor of muscle fiber growth[49; 50], and future work will determine if myonuclear accrual following ACL reconstruction is predictive of positive rehabilitation outcomes.

A limitation of this study was that we studied patients at a single time point following their ACL injury using immunohistochemical analyses. Longitudinal analysis of the maladaptations that occur within skeletal muscle would provide greater detail than the single point captured in the current manuscript allows. Understanding the time course of deleterious changes that occur in the muscle following an ACL tear would help to establish the progression of physiological adaptations and provide greater detail regarding potential mechanisms. Future studies will also seek to distinguish phenotypic differences in Tcf4+ and PDGFRα+ cells, as well as biochemical assessment of alterations within the muscle ECM. Additionally, inactivity and unloading have been shown to induce a program of deleterious morphological adaptations within skeletal muscle[28; 51; 52]. While subjects' were completely weight-bearing at the time of data collection in the current study, we cannot completely eliminate a potential contribution of inactivity/loading on the observed muscle adaptations following ACL injury.

In conclusion, injury and reconstruction of the ACL induces a myriad of negative outcomes within knee extensor muscles, including collagen accumulation, increased fibroblast and FAP content in addition to reduced satellite cell abundance. Alterations in the interstitial environment surrounding muscle fibers and a reduced satellite cell pool likely compromise the restorative capacity of skeletal muscle and impede rehabilitative efforts. A greater understanding of skeletal muscle maladaptation following ACL injury will hopefully improve rehabilitation and lead to the development of therapies that directly target protracted muscle weakness.

Acknowledgments

CSF is a KL2 scholar supported by the UTMB Claude D. Pepper Older Americans Independence Center NIH/NIA grant P30 AG024832. BN is supported by the National Institute of Arthritis and Musculoskeletal and Skin Diseases of the National Institutes of Health under Award Number K23 AR062069. The content is solely the responsibility of the authors and does not necessarily represent the official views of the National Institutes of Health

References

1. Griffin LY, Albohm MJ, Arendt EA, et al. Understanding and preventing noncontact anterior cruciate ligament injuries: a review of the Hunt Valley II meeting, January 2005. Am J Sports Med. 2006; 34:1512–1532. [PubMed: 16905673]
2. McLean SG, Beaulieu ML. Complex integrative morphological and mechanical contributions to ACL injury risk. Exercise and Sport Science Reviews. 2010; 38:192–200.
3. Hiemstra LA, Webber S, MacDonald PB, et al. Knee strength deficits after hamstring tendon and patellar tendon anterior cruciate ligament reconstruction. Medicine Science Sports Exercise. 2000; 32:1472–1479.
4. DeVita P, Hortobagyi T, Barrier J. Gait biomechanics are not normal after anterior cruciate ligament reconstruction and accelerated rehabilitation. Medicine Science Sports Exercise. 1998; 30:1481–1488.
5. Paterno MV, Ford KR, Myer GD, et al. Limb asymmetries in landing and jumping 2 years following anterior cruciate ligament reconstruction. Clinical Journal Sport Medicine. 2007; 17:258–262.
6. Bryant AL, Kelly J, Hohmann E. Neuromuscular adaptations and correlates of knee functionality following ACL reconstruction. J Orthop Res. 2008; 26:126–135. [PubMed: 17676614]
7. Webster KE, Feller JA. Alterations in joint kinematics during walking following hamstring and patellar tendon anterior cruciate ligament reconstruction surgery. Clinical Biomechanics. 2011; 26:175–180. [PubMed: 20950901]
8. Feller JA, Webster KE. A Randomized Comparison of Patellar Tendon and Hamstring Tendon Anterior Cruciate Ligament Reconstruction. The American Journal of Sports Medicine. 2003; 31:564–573. [PubMed: 12860546]
9. Jansson KA, Linko E, Sandelin J, et al. A prospective randomized study of patellar versus hamstring tendon autografts for anterior cruciate ligament reconstruction. Am J Sports Med. 2003; 31:12–18. [PubMed: 12531751]
10. Maletis GB, Cameron SL, Tengan JJ, et al. A prospective randomized study of anterior cruciate ligament reconstruction: a comparison of patellar tendon and quadruple-strand semitendinosus/gracilis tendons fixed with bioabsorbable interference screws. Am J Sports Med. 2007; 35:384–394. [PubMed: 17218661]
11. Natri A, Jarvinen M, Latvala K, et al. Isokinetic muscle performance after anterior cruciate ligament surgery. Long-term results and outcome predicting factors after primary surgery and late-phase reconstruction. Int J Sports Med. 1996; 17:223–228. [PubMed: 8739578]
12. Palmieri-Smith RM, Thomas AC, Wojtys EM. Maximizing quadriceps strength after ACL reconstruction. Clin Sports Med. 2008; 27:405–424. vii–ix. [PubMed: 18503875]
13. Snyder-Mackler L, Delitto A, Bailey SL, et al. Strength of the quadriceps femoris muscle and functional recovery after reconstruction of the anterior cruciate ligament. A prospective, randomized clinical trial of electrical stimulation. J Bone Joint Surg Am. 1995; 77:1166–1173. [PubMed: 7642660]
14. Witvrouw E, Bellemans J, Verdonk R, et al. Patellar tendon vs. doubled semitendinosus and gracilis tendon for anterior cruciate ligament reconstruction. Int Orthop. 2001; 25:308–311. [PubMed: 11794266]
15. Lindström M, Strandberg S, Wredmark T, et al. Functional and muscle morphometric effects of ACL reconstruction. A prospective CT study with 1 year follow-up. Scand J Med Sci Sports. 2011 n/a-n/a.

16. Ardern CL, Taylor NF, Feller JA, et al. Return-to-Sport Outcomes at 2 to 7 Years After Anterior Cruciate Ligament Reconstruction Surgery. The American Journal of Sports Medicine. 2012; 40:41–48. [PubMed: 21946441]
17. Noehren B, Andersen A, Hardy P, Johnson DR, Ireland ML, Thompson KL, Damon B. Cellular and Morphological Alterations in the Vastus Lateralis Muscle as the Result of ACL Injury and Reconstruction. J Bone Joint Surg Am. 2016 In press.
18. Fry CS, Lee JD, Jackson JR, et al. Regulation of the muscle fiber microenvironment by activated satellite cells during hypertrophy. Faseb Journal. 2014; 28:1654–1665. [PubMed: 24376025]
19. Zou Y, Zhang RZ, Sabatelli P, et al. Muscle interstitial fibroblasts are the main source of collagen VI synthesis in skeletal muscle: Implications for congenital muscular dystrophy types Ullrich and Bethlem. Journal of Neuropathology and Experimental Neurology. 2008; 67:144–154. [PubMed: 18219255]
20. Murphy MM, Lawson JA, Mathew SJ, et al. Satellite cells, connective tissue fibroblasts and their interactions are crucial for muscle regeneration. Development. 2011; 138:3625–3637. [PubMed: 21828091]
21. Uezumi A, Ito T, Morikawa D, et al. Fibrosis and adipogenesis originate from a common mesenchymal progenitor in skeletal muscle. Journal of Cell Science. 2011; 124:3654–3664. [PubMed: 22045730]
22. Dulauroy S, Di Carlo SE, Langa F, et al. Lineage tracing and genetic ablation of ADAM12(+) perivascular cells identify a major source of profibrotic cells during acute tissue injury. Nat Med. 2012; 18:1262–1270. [PubMed: 22842476]
23. Olson LE, Soriano P. Increased PDGFRalpha activation disrupts connective tissue development and drives systemic fibrosis. Developmental cell. 2009; 16:303–313. [PubMed: 19217431]
24. Fry CS, Noehren B, Mula J, et al. Fibre type-specific satellite cell response to aerobic training in sedentary adults. J Physiol. 2014; 592:2625–2635. [PubMed: 24687582]
25. Fry CS, Porter C, Sidossis LS, et al. Satellite cell activation and apoptosis in skeletal muscle from severely burned children. J Physiol. 2016
26. Liu F, Fry CS, Mula J, et al. Automated fiber-type-specific cross-sectional area assessment and myonuclei counting in skeletal muscle. Journal of Applied Physiology. 2013; 115:1714–1724. [PubMed: 24092696]
27. Uezumi A, Fukada S, Yamamoto N, et al. Identification and characterization of PDGFRalpha+ mesenchymal progenitors in human skeletal muscle. Cell Death Dis. 2014; 5:e1186. [PubMed: 24743741]
28. Arentson-Lantz EJ, English KL, Paddon-Jones D, et al. Fourteen days of bed rest induces a decline in satellite cell content and robust atrophy of skeletal muscle fibers in middle-aged adults. J Appl Physiol. 2016; 120:965–975. 1985. [PubMed: 26796754]
29. Verdijk LB, Snijders T, Drost M, et al. Satellite cells in human skeletal muscle; from birth to old age. Age (Dordr). 2013
30. Andersson AM, Olsen M, Zhernosekov D, et al. Age-related changes in expression of the neural cell adhesion molecule in skeletal muscle: a comparative study of newborn, adult and aged rats. Biochem J. 1993; 290(Pt 3):641–648. [PubMed: 8457191]
31. Gosztonyi G, Naschold U, Grozdanovic Z, et al. Expression of Leu-19 (CD56, N-CAM) and nitric oxide synthase (NOS) I in denervated and reinnervated human skeletal muscle. Microsc Res Tech. 2001; 55:187–197. [PubMed: 11747094]
32. Meyer GA, Ward SR. Developmental Biology and Regenerative Medicine: Addressing the Vexing Problem of Persistent Muscle Atrophy in the Chronically Torn Human Rotator Cuff. Phys Ther. 2016
33. Urciuolo A, Quarta M, Morbidoni V, et al. Collagen VI regulates satellite cell self-renewal and muscle regeneration. Nat Commun. 2013; 4:1964. [PubMed: 23743995]
34. Gilbert PM, Havenstrite KL, Magnusson KEG, et al. Substrate Elasticity Regulates Skeletal Muscle Stem Cell Self-Renewal in Culture. Science. 2010; 329:1078–1081. [PubMed: 20647425]
35. Brack AS, Rando TA. Intrinsic changes and extrinsic influences of myogenic stem cell function during aging. Stem Cell Rev. 2007; 3:226–237. [PubMed: 17917136]

36. Mann CJ, Perdiguero E, Kharraz Y, et al. Aberrant repair and fibrosis development in skeletal muscle. Skelet Muscle. 2011; 1:21. [PubMed: 21798099]
37. Uezumi A, Fukada S, Yamamoto N, et al. Mesenchymal progenitors distinct from satellite cells contribute to ectopic fat cell formation in skeletal muscle. Nat Cell Biol. 2010; 12
38. Farup J, De Lisio M, Rahbek SK, et al. Pericyte response to contraction mode-specific resistance exercise training in human skeletal muscle. J Appl Physiol. 2015; 119:1053–1063. 1985. [PubMed: 26404620]
39. Joe AWB, Yi L, Natarajan A, et al. Muscle injury activates resident fibro/adipogenic progenitors that facilitate myogenesis. Nature Cell Biology. 2010; 12:153–163. [PubMed: 20081841]
40. Mathew SJ, Hansen JM, Merrell AJ, et al. Connective tissue fibroblasts and Tcf4 regulate myogenesis. Development. 2011; 138:371–384. [PubMed: 21177349]
41. Murphy MM, Lawson JA, Mathew SJ, et al. Satellite cells, connective tissue fibroblasts and their interactions are crucial for muscle regeneration. Development. 2011; 138:3625–3637. [PubMed: 21828091]
42. Uezumi A, Ikemoto-Uezumi M, Tsuchida K. Roles of nonmyogenic mesenchymal progenitors in pathogenesis and regeneration of skeletal muscle. Front Physiol. 2014; 5:68. [PubMed: 24605102]
43. Montesano R, Orci L. TRANSFORMING GROWTH FACTOR-BETA STIMULATES COLLAGEN-MATRIX CONTRACTION BY FIBROBLASTS - IMPLICATIONS FOR WOUND-HEALING. Proceedings of the National Academy of Sciences of the United States of America. 1988; 85:4894–4897. [PubMed: 3164478]
44. McCarthy JJ, Mula J, Miyazaki M, et al. Effective fiber hypertrophy in satellite cell-depleted skeletal muscle. Development. 2011; 138:3657–3666. [PubMed: 21828094]
45. Moss FP, Leblond CP. Satellite cells as the source of nuclei in muscles of growing rats. Anat Rec. 1971; 170:421–435. [PubMed: 5118594]
46. Amthor H, Otto A, Vulin A, et al. Muscle hypertrophy driven by myostatin blockade does not require stem/precursor-cell activity. Proceedings of the National Academy of Sciences of the United States of America. 2009; 106:7479–7484. [PubMed: 19383783]
47. Fry CS, Kirby TJ, Kosmac K, et al. Myogenic Progenitor Cells Control Extracellular Matrix Production by Fibroblasts during Skeletal Muscle Hypertrophy. Cell Stem Cell. 2016 epub ahead of print.
48. Messi ML, Li T, Wang ZM, et al. Resistance Training Enhances Skeletal Muscle Innervation Without Modifying the Number of Satellite Cells or their Myofiber Association in Obese Older Adults. J Gerontol A Biol Sci Med Sci. 2015; 71:1273–1280. [PubMed: 26447161]
49. Petrella JK, Kim JS, Cross JM, et al. Efficacy of myonuclear addition may explain differential myofiber growth among resistance-trained young and older men and women. American Journal of Physiology-Endocrinology and Metabolism. 2006; 291:E937–E946. [PubMed: 16772322]
50. Petrella JK, Kim J-S, Mayhew DL, et al. Potent myofiber hypertrophy during resistance training in humans is associated with satellite cell-mediated myonuclear addition: a cluster analysis. Journal of Applied Physiology. 2008; 104:1736–1742. [PubMed: 18436694]
51. Leeuwenburgh C, Gurley CM, Strotman BA, et al. Age-related differences in apoptosis with disuse atrophy in soleus muscle. Am J Physiol Regul Integr Comp Physiol. 2005; 288:R1288–R1296. [PubMed: 15650125]
52. Wang XD, Kawano F, Matsuoka Y, et al. Mechanical load-dependent regulation of satellite cell and fiber size in rat soleus muscle. Am J Physiol Cell Physiol. 2006; 290:C981–C989. [PubMed: 16291821]

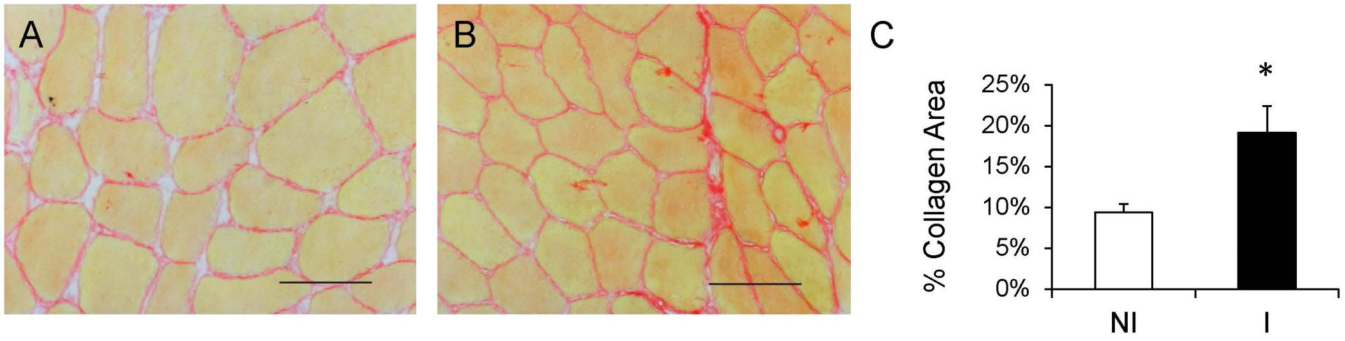

Figure 1. Increased muscle collagen accumulation following ACL injury

(A–B) Representative images showing collagen (red) staining in the non-injured (A) and injured (B) limb skeletal muscle. Scale bar = 50μm. C) Quantification of muscle collagen content presented as mean percentage of total muscle area ± SEM. N = 10 subjects. NI = non-injured; I = injured. * Significantly different from the non-injured limb ($p < 0.05$).

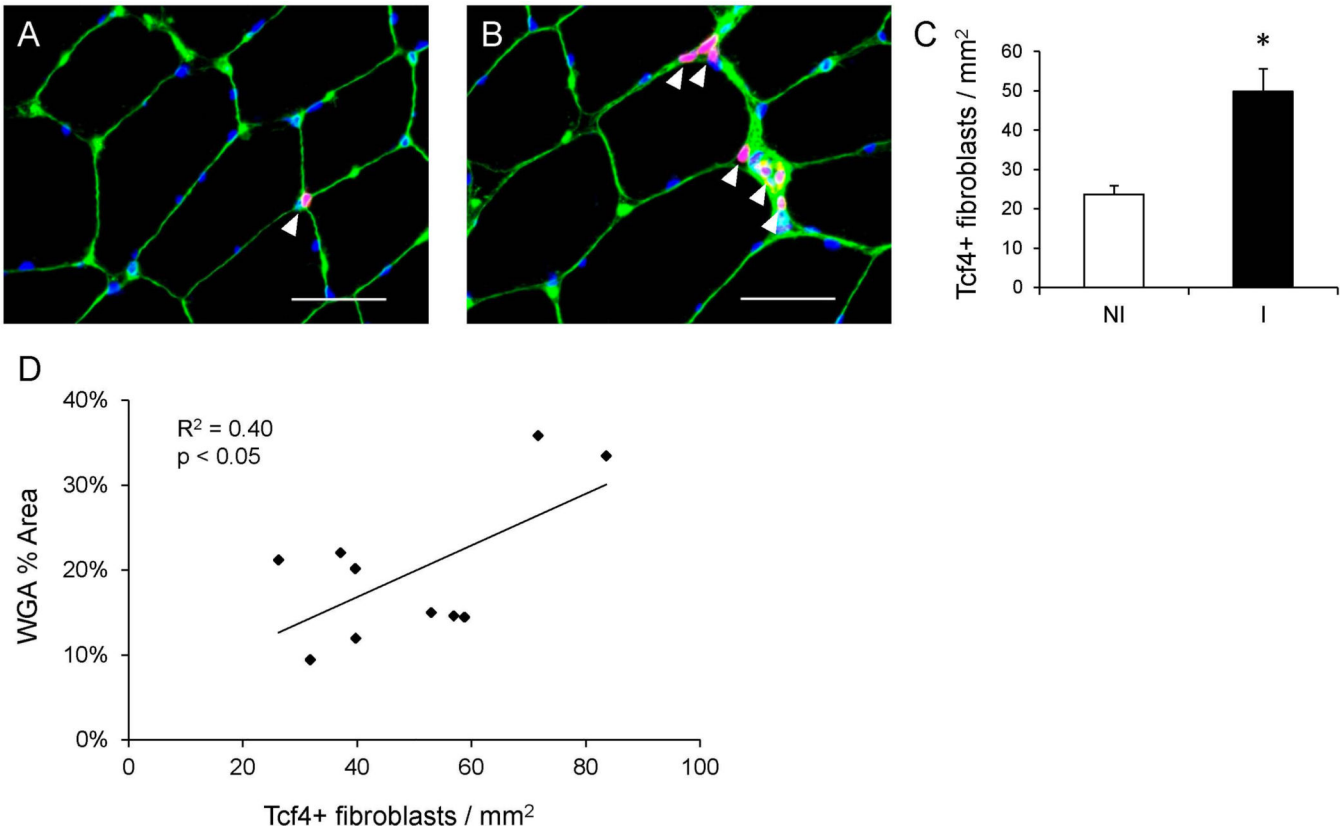

Figure 2. ACL injury induces increased connective tissue fibroblast abundance in skeletal muscle

(A–B) Representative immunohistochemical images demonstrating Tcf4+ connective tissue fibroblasts (white arrowheads, red), muscle connective tissue (green), and DAPI (blue) in the non-injured (A) and injured (B) limb skeletal muscle. Scale bar = 50μm. (C) Quantification of Tcf4+ fibroblasts presented as mean number of fibroblasts per muscle area (mm^2) ± SEM. (D) Correlation of the number of fibroblasts per mm^2 with percent area of muscle connective tissue in the injured limb. N = 10 subjects. NI = non-injured; I = injured. * Significantly different from the non-injured limb ($p < 0.05$).

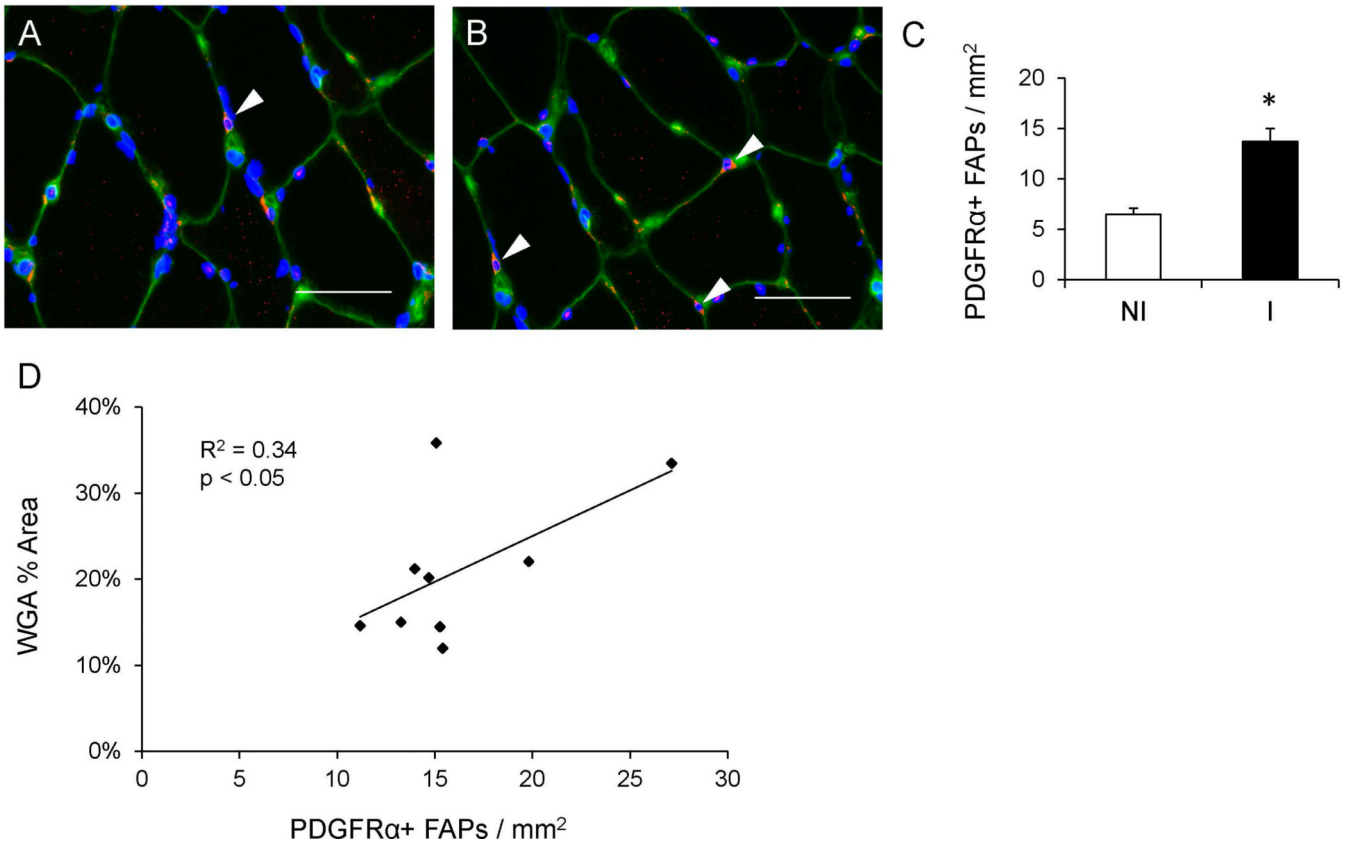

Figure 3. Elevated number of fibrogenic/adipogenic progenitor (FAP) cells in the muscle following an ACL injury

(A–B) Representative immunohistochemical images demonstrating PDGFRα+ FAPs (white arrowheads, red), muscle connective tissue (green), and DAPI (blue) in the non-injured (A) and injured (B) limb skeletal muscle. Scale bar = 50μm. (C) Quantification of PDGFRα+ FAPs presented as mean number of FAPs per muscle area (mm^2) ± SEM. (D) Correlation of the number of FAPs per mm^2 with percent area of muscle connective tissue in the injured limb. N = 9 subjects. NI = non-injured; I = injured. * Significantly different from the non-injured limb ($p < 0.05$).

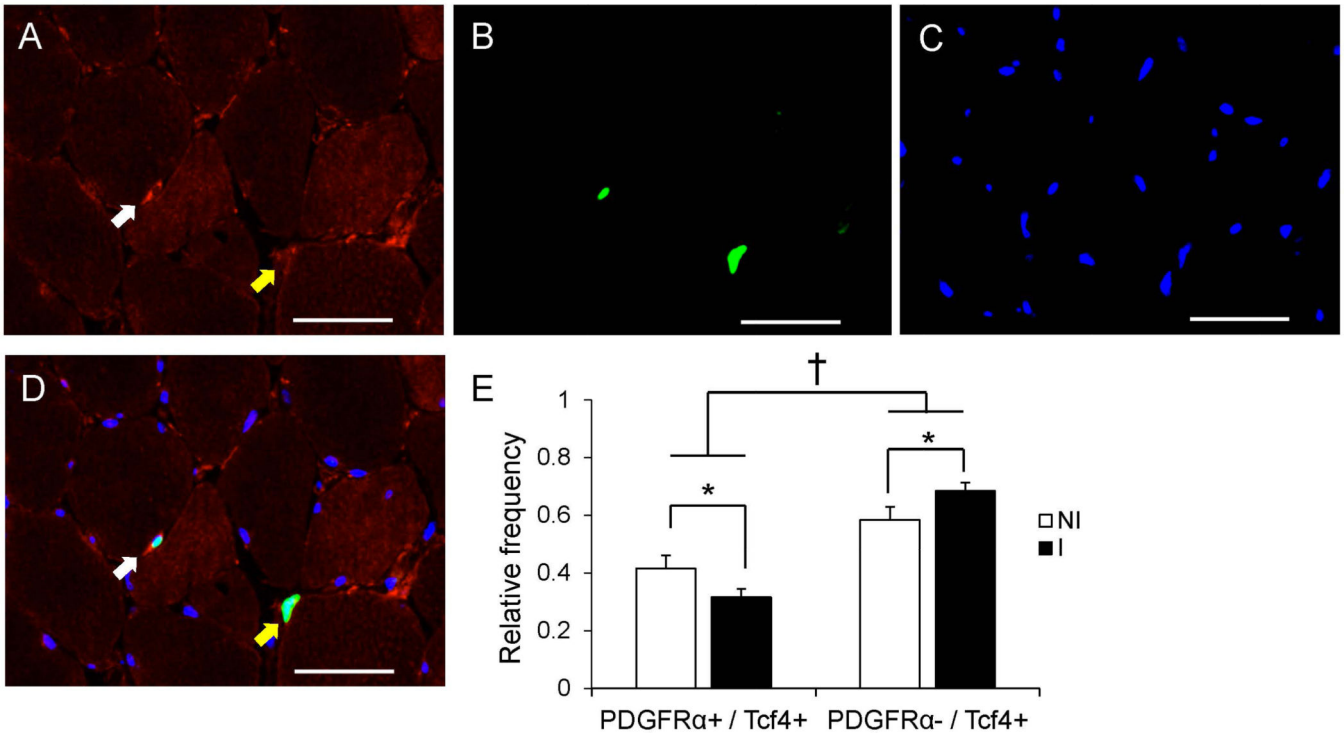

Figure 4. PDGFRα+ and Tcf4+ co-localization is affected by ACL injury

Representative images of PDGFRα (A), Tcf4 (B) and DAPI (C) staining in ACL injured muscle. (D) Merged immunohistochemical image demonstrating a PDGFRα+ / Tcf4+ cell (white arrow) and a PDGFRα− / Tcf4+ cell (yellow arrow). Scale bar = 50μm. (E) Quantification presented as mean relative frequency of cells staining for both PDGFRα and Tcf4 versus Tcf4 alone ± SEM. * Significantly different from the non-injured limb ($p < 0.05$); † Significant effect of PDGFRα-staining status ($p < 0.05$).

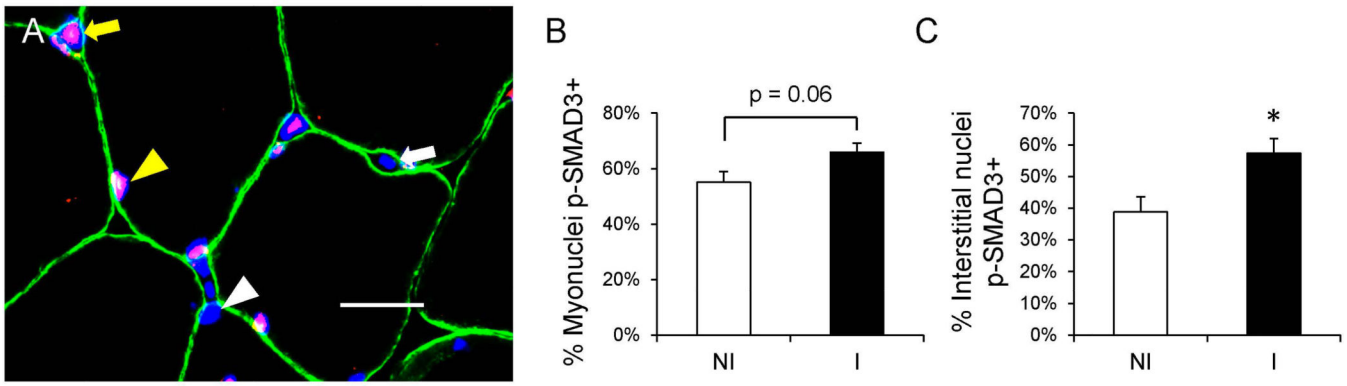

Figure 5. Increased frequency of p-SMAD3+ nuclei in the skeletal muscle following ACL injury

(A) Representative immunohistochemical image demonstrating p-SMAD3 (red), dystrophin (green), and DAPI (blue) in the non-injured limb skeletal muscle. A white arrowhead denotes a p-SMAD3− myonucleus, a yellow arrowhead denotes a p-SMAD3+ myonucleus, a white arrow denotes a p-SMAD3− interstitial nucleus and a yellow arrow denotes a p-SMAD3+ interstitial nucleus. Scale bar = 20μm. (B) Quantification of the frequency of p-SMAD3 myonuclei, expressed as mean percentage of p-SMAD3+ myonuclei ± SEM. (C) Quantification of the frequency of p-SMAD3 interstitial nuclei, expressed as mean percentage of p-SMAD3+ interstitial nuclei ± SEM. N = 10 subjects. NI = non-injured; I = injured. * Significantly different from the non-injured limb ($p < 0.05$).

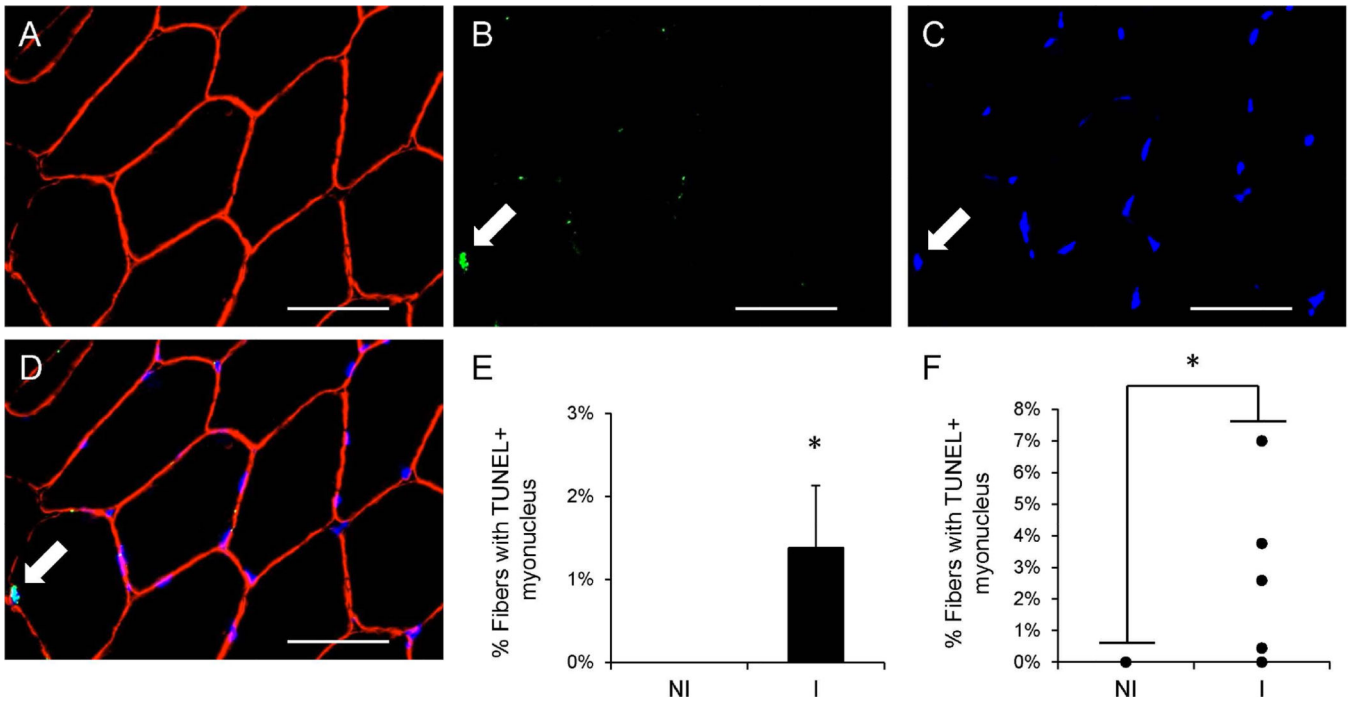

Figure 6. Myonuclear apoptosis increases following ACL injury

Representative images of dystrophin (A), TUNEL (B) and DAPI (C) staining in ACL injured muscle. (D) Merged immunohistochemical image demonstrating a TUNEL+ myonucleus (white arrow). Scale bar = 50μm. (E) Quantification presented as mean percentage of fibers with a TUNEL+ myonucleus ± SEM. (F) Quantification of individual subject TUNEL+ myonuclei fiber frequency data. N = 10 subjects. NI = non-injured; I = injured. * Significantly different from the non-injured limb ($p < 0.05$).

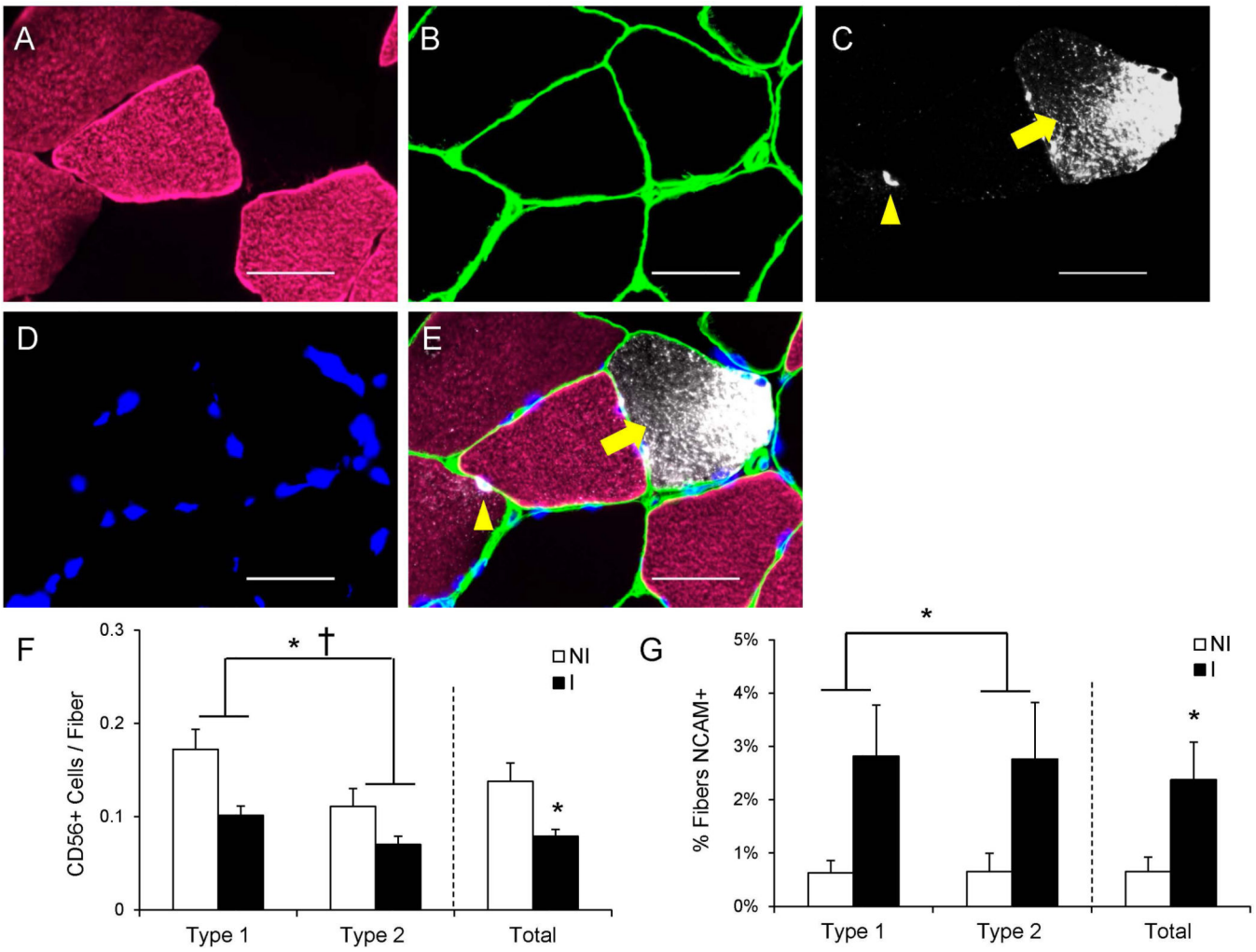

Figure 7. Reduced satellite cell abundance and increased frequency of muscle fiber denervation following ACL injury

(A–D) Representative images of myosin heavy chain type 1 (A), laminin (B), CD56/Neural Cell Adhesion Molecule (NCAM) (C) and DAPI (D) staining in ACL injured muscle. (E) Merged immunohistochemical image demonstrating a CD56+ satellite cell (yellow arrowhead) and a NCAM+ muscle fiber (yellow arrow). Scale bar = 50μm. (F) Quantification of fiber type-specific and pooled CD56+ satellite cell content, expressed as mean CD56+ satellite cells per fiber ± SEM. (G) Quantification of fiber type-specific and pooled NCAM+ fibers, expressed as mean percentage of fibers positive for NCAM ± SEM. N = 10 subjects. NI = non-injured; I = injured. * Significantly different from the non-injured limb ($p < 0.05$); † Significant effect of fiber type ($p < 0.05$).